Mustang Fall 2006 Engineering Run Results

Brian Mason, Simon Dicker, Phil Korngut, & James Aguirre

v.1 March 7, 2007

1. Introduction

MUSTANG was installed on the GBT in September of 2006 for a 2-month commissioning run, the goals of which were:

- to verify basic functionality of the optics;
- to verify basic functionality of the detector array;
- to identify problems uniquely inherent to the telescope environment (e.g., magnetic fields or microphonics);
- and to fully exercise the system as a whole for the first time.

A number of risks and challenges were expected going into this run. Notably: the GBT aperture efficiency at 90 GHz was unknown (expected to be ~ 5-15%); the detector noise levels in the lab were roughly 100 times the target noise levels (dominated by a large 1/f noise component); and a number of last-minute changes to the hardware were necessary immediately prior to the run (principally removing inductors in the SQUID MUX circuit and replacing a delaminated bandpass filter). On the whole, and in spite of these challenges, the run was extremely successful.

This memo documents other aspects of the run and our main findings from it. An accompanying memo ("Fall 2006: Cryogenics on the GBT") characterizes in more detail the cryogenic performance of MUSTANG on the GBT, and subsequent diagnostics in the lab. A further memo of interest as pertains detector performance is "Mustang detectors—Array 2", laying out an exhaustive characterization of detector noise properties in the commissioning run and subsequent lab investigations leading up to the Feb 9th 2007 detector review meeting at NASA GSFC.

2. Summary of Data

Data were collected in 8 sessions , briefly described as follows:

- TPAR_01 (21sep) – marginal hints of signals from bright calibrators were seen—we were still figuring out how to focus the telescope (collect and appropriately analyze the data, apply focus corrections, etc).
- TPAR_02 (26sep) – successful first light observations!
- TPAR_03 (04oct) – late start owing to punishing observer (long dwells at low elevation heated up the dewar); crate problem at the end of the night.
- TPAR_04 (13oct)-- late start; long run; observed many sources but best active-surface model not on at start of run.

- TPAR_05 (19oct)-- good observations of 3c84; Saturn OOF map.
- TPAR_06 (21oct)-- beammap observations.
- TPAR_07 (26oct)-- MUSTANG never got cold. Night spent collecting K-band maps of bright sources.
- TPAR_08 (09nov)-- system functioned well; poor weather.

3. Functioning/Non-functioning Detectors

Roughly half of the detectors were seen to respond to light (the internal noise calibration source); a typical array response to the flashing cal signal is shown in the following figure. Of these about 8 detectors typically showed gross instabilities rendering them unusable. Of the remaining ~24, noise levels between them were quite variable (between detectors and over time) and some form of detector weights are an essential step to obtain useful maps of the sky.

Some notes on individual detectors and columns:

- c0r2, c0r3, c1r0, c5r2, & c5r4 are consistently nonresponsive, or weakly responsive with the opposite sign as the rest of the column. We think c5r2 is the pixel sacrificed for G measurement.
- c5r5 consistently shows a weak response (but not as weak) that is opposite in sign to the rest of the column.
- Detectors which not infrequently show gross instabilities are: c1r3, c1r4, c2r0, c2r3, c4r1, c4r2, c4r3, c4r5, c4r6, c5r0, c5r3, c6r5.
- Column 3 had a poorly heat-sunk series array and was rarely used in observations. Column 7 had a detector bias line with a cold open circuit condition which has since been fixed.

No obvious correlation between grossly noisy pixels and shunt resistance or measured Tc's is seen. Anomalous shunt resistances do explain most of the “dead” detectors (c0r2 and c0r3 have Rshunts 2x bigger than others in the column; c5r4 has Rshunt 2x lower than others in the column; c1r0 has Rshunt 25+ % lower than the others in the column).

Cal Light Curves (Figure 5) illustrating these properties can be seen in the next section (Figure 5)

We also note some properties of the wiring:

- alternate columns have opposite response to power
- Column 5 has its rows wired backwards

4. Shunt Resistor Values

In the lab at Green Bank the shunt resistances were measured for the whole array. This was done by measuring the Johnson current noise I_rms (in Amps per root Hz) noise across each shunt resistor with its TES in the superconducting state. These data were acquired in a standard MUXing mode and calibrated to amps using equations in Section 6. We calculate the shunt resistances using the relation

$$r_{shunt} = 4kT / I_{rms}^2$$

where T is the physical temperature of the resistor (all assumed equal to the measured temperature at the focal plane). Results ,in milliohms and laid out by logical row and column, are:

0.91	1.5	1.6	--	1.6	1.9	1.4	--
0.9	1.5	1.6	--	1.6	1.9	1.4	--
2.3	1.2	1.6	--	1.7	12.0	1.3	--
2.5	1.2	1.6	--	1.7	1.8	1.5	--
1.1	1.2	1.5	--	1.7	0.6	1.4	--
1.2	1.2	1.7	--	1.8	1.2	1.4	--
1.2	1.2	1.7	--	1.6	1.9	1.4	--
1.3	1.4	1.7	--	1.9	2.0	1.3	--

Anomalous values for a given column are highlighted.

5. Receiver Optics

Due to the high noise levels present in the data, most optical characterization measurements could only be done using Saturn, which is highly resolved (a 15" diameter disk). Using these data we were able to measure individual pixel beam offsets (Figures 1 & 2) . High signal-to-noise ratio observations of point sources are desirable to characterize the point spread function for individual detectors in detail. The high noise levels of the receiver and low surface efficiency of the GBT prevented acquiring such data. However, the beam properties derived from analyzing images (formed by coadding all the detectors' data) of quick Saturn maps made at a range of focus settings are qualitatively reasonable (Figure 3).

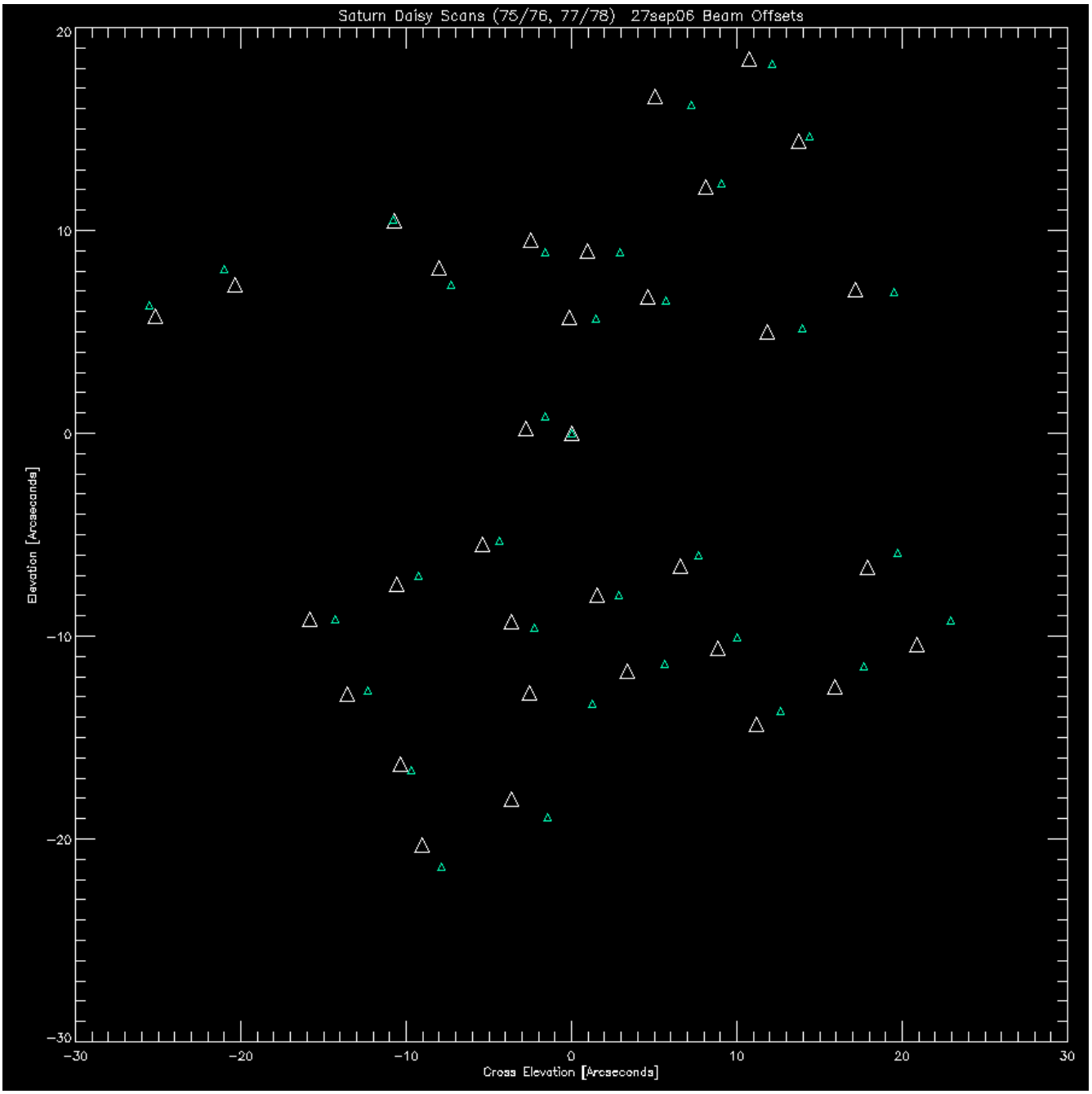

FIGURE 1: Individual pixel elevation and cross-elevation offsets on the sky in arcseconds determined from fitting daisy scans on Saturn (27sep06). Green and white are determinations from two successive scans within 10 minutes; some systematic pointing wander is evident.

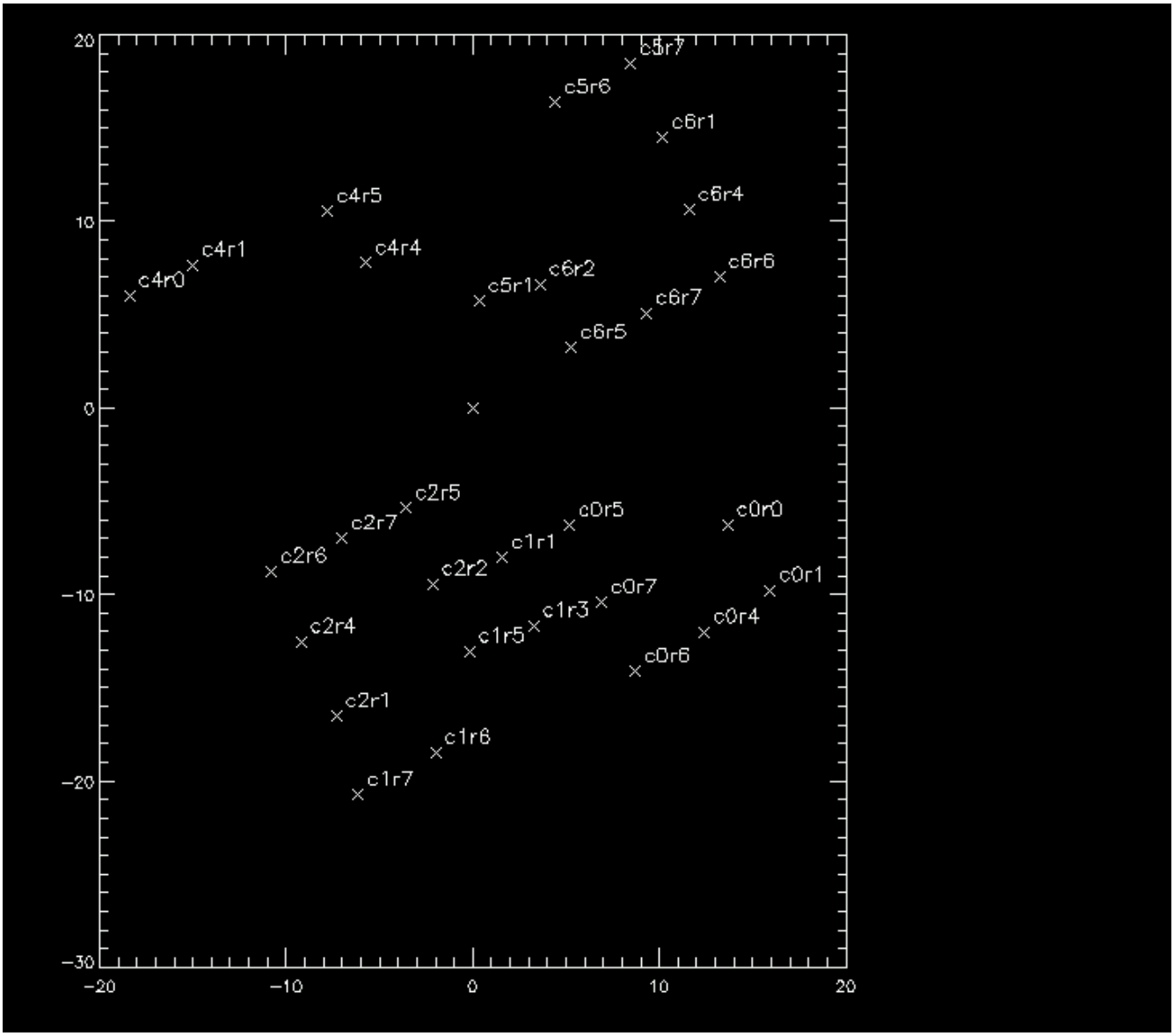

FIGURE 2: Individual detector offsets identified by colun and row.

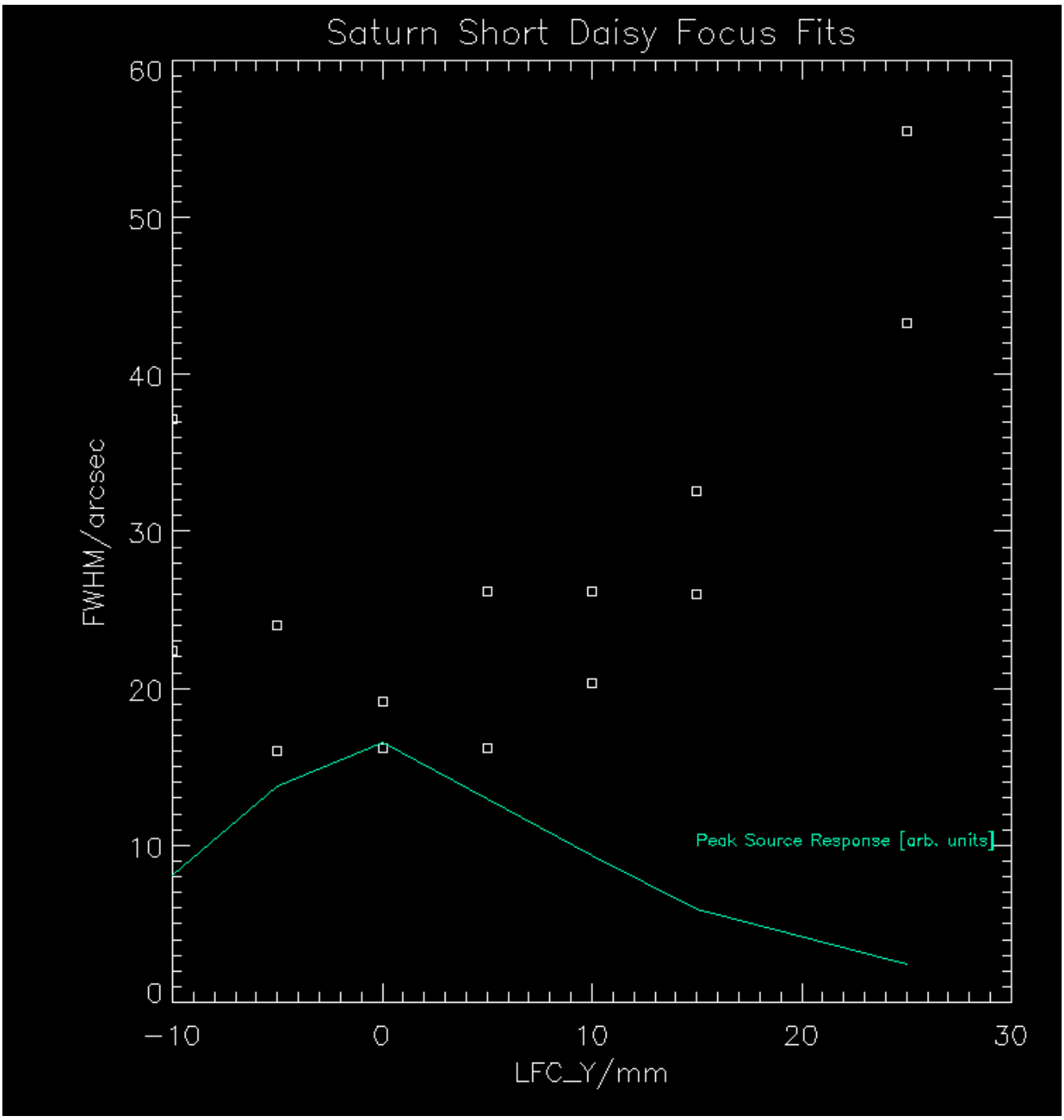

FIGURE 3: Results of beam fits to focus scans on Saturn, showing major and minor axis of the fit in arcseconds and fitted peak source response.

6. Noise Characteristics

Following are noise power spectra on the telescope and in the lab, under a range of conditions. Data were calibrated from DAC counts to current fluctuations (in Amps) using the relation

$$\Delta I = \Delta dac \text{ x } \frac{\Phi_0}{DAC} \text{ x } \frac{Amps}{\Phi_0}$$

Here DAC/Phi0 (the reciprocal of the factor above) is typically 4000 +/- 20%, but can be measured for each detector from the firmware ramps (sweeping the DAC and measuring the period of the SAE response). Amps/Phi0 is a geometrical constant characteristic of the first stage SQUIDS. The constant is provided by NIST (we use 6 microAmps/phi0).

Current fluctuations are converted to fluctuations in power as

$$\Delta P = \Delta I \text{ x Q B x } \frac{r_S}{R}$$

where: Q is the (bias line) digital-to-analog converter's volts-per-count value (37 microVolts per count); B is the column bias voltage in counts; r_s is the shunt resistance for the given detector loop, measured from the Johnson noise; and R is the input resistance (1 kOhm for this run).

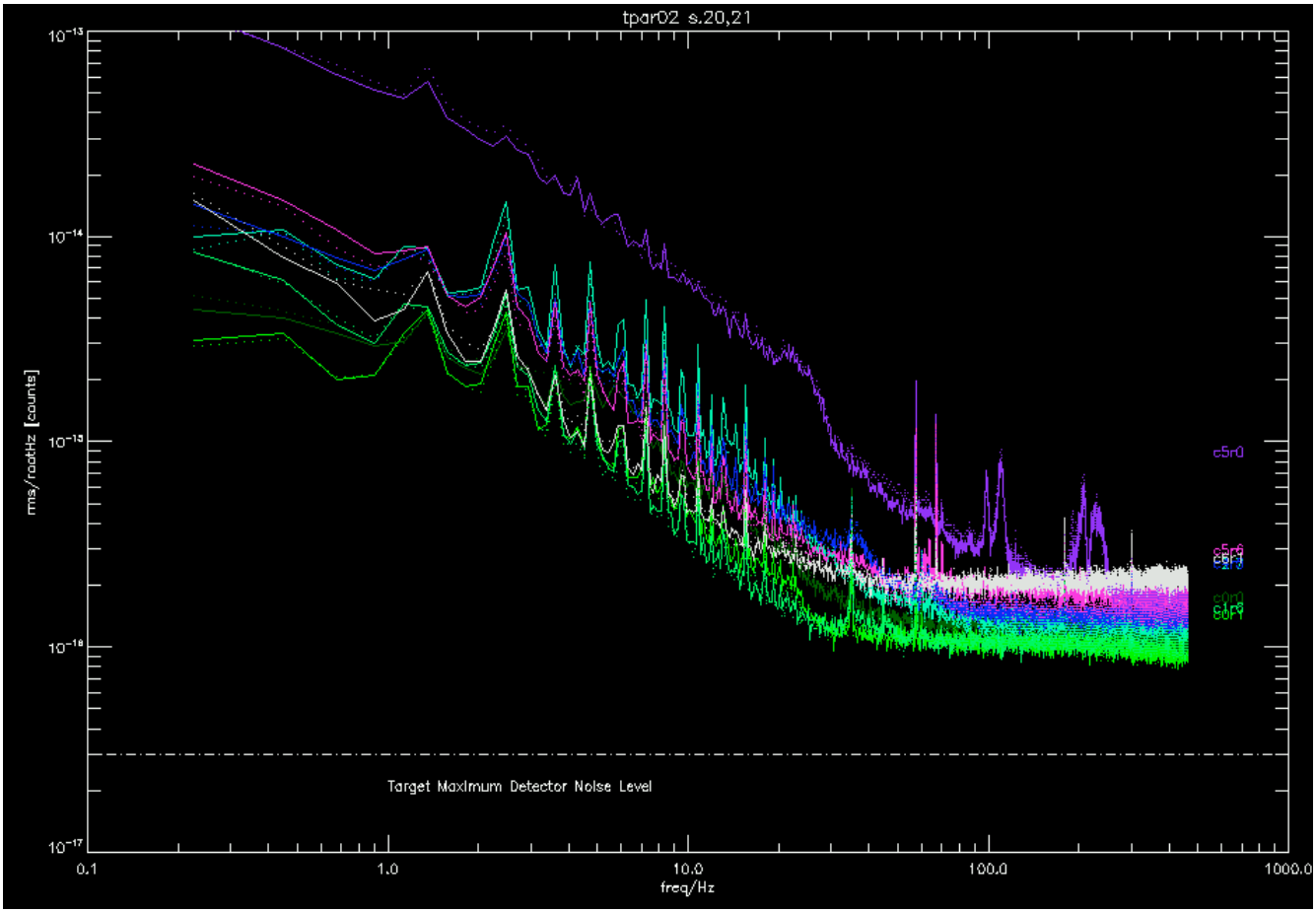

FIGURE 4: Noise power spectra from a representative set of detectors collected on the GBT (TPAR02; scans 20 (solid) and 21 (dotted)). Some of these are 'good' detectors and some (eg c5r0) show obvious instabilities in the Cal light curves. Y-axis is in Watts-rtHz.

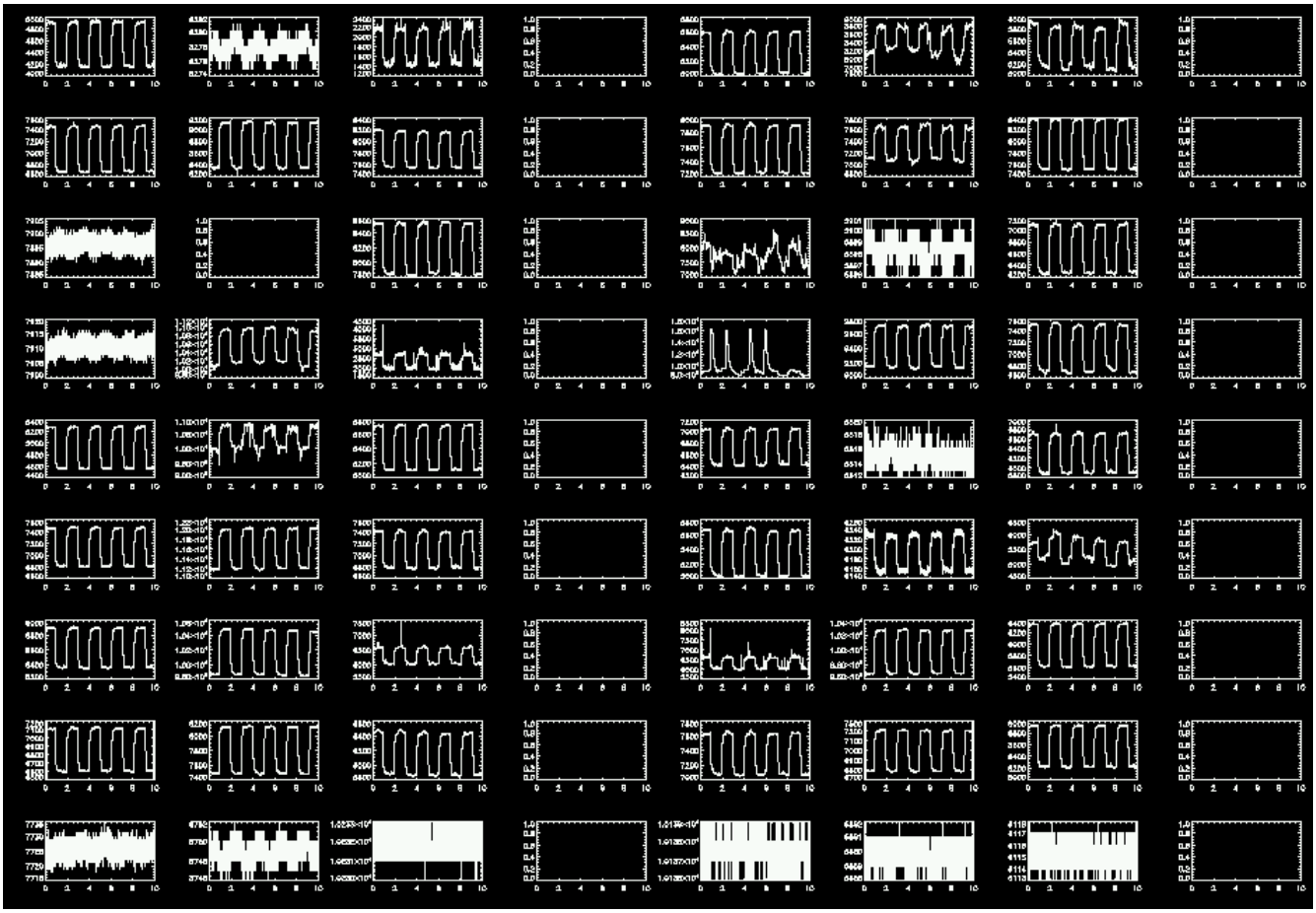

FIGURE 5: Cal light curves for TPAR02, scan 19, with the same biases as in the TPAR02 power spectrum plot. Individual panels are layed out by LOGICAL column and row in this figure. The bottom row is the dark SQUIDs; the consistently non-responsive c0r2, c0r3, c5r2, & c5r4 pixels identified previously can also be seen. C5r5 can also be seen to have the opposite sign to the rest of the column.

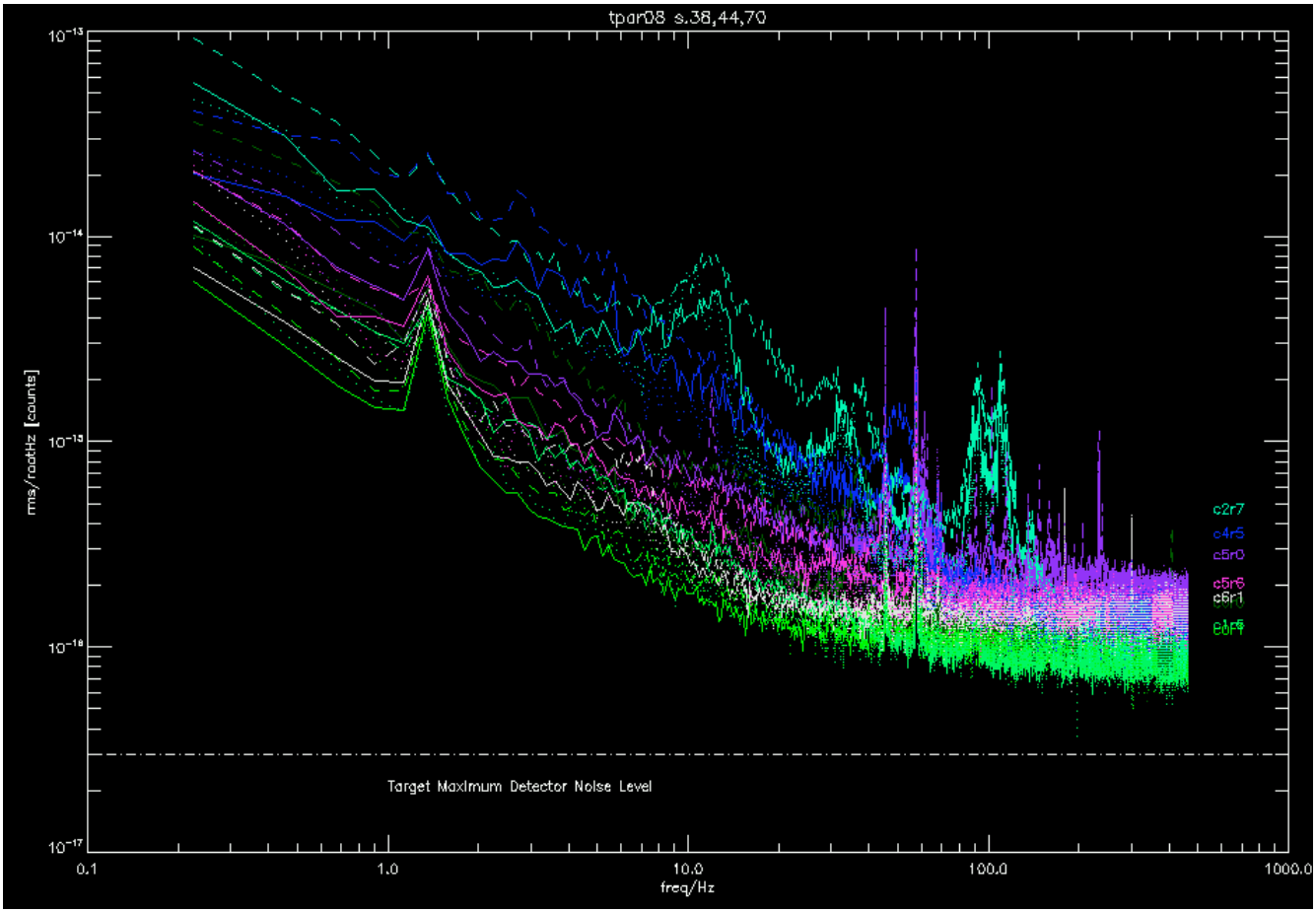

FIGURE 6: A set of representative power spectra for 3 scans from TPAR08. Y-axis is in Watts rtHz. As in Figure 4, some of these are "good" pixels, and some show obvious light-curve instabilities.

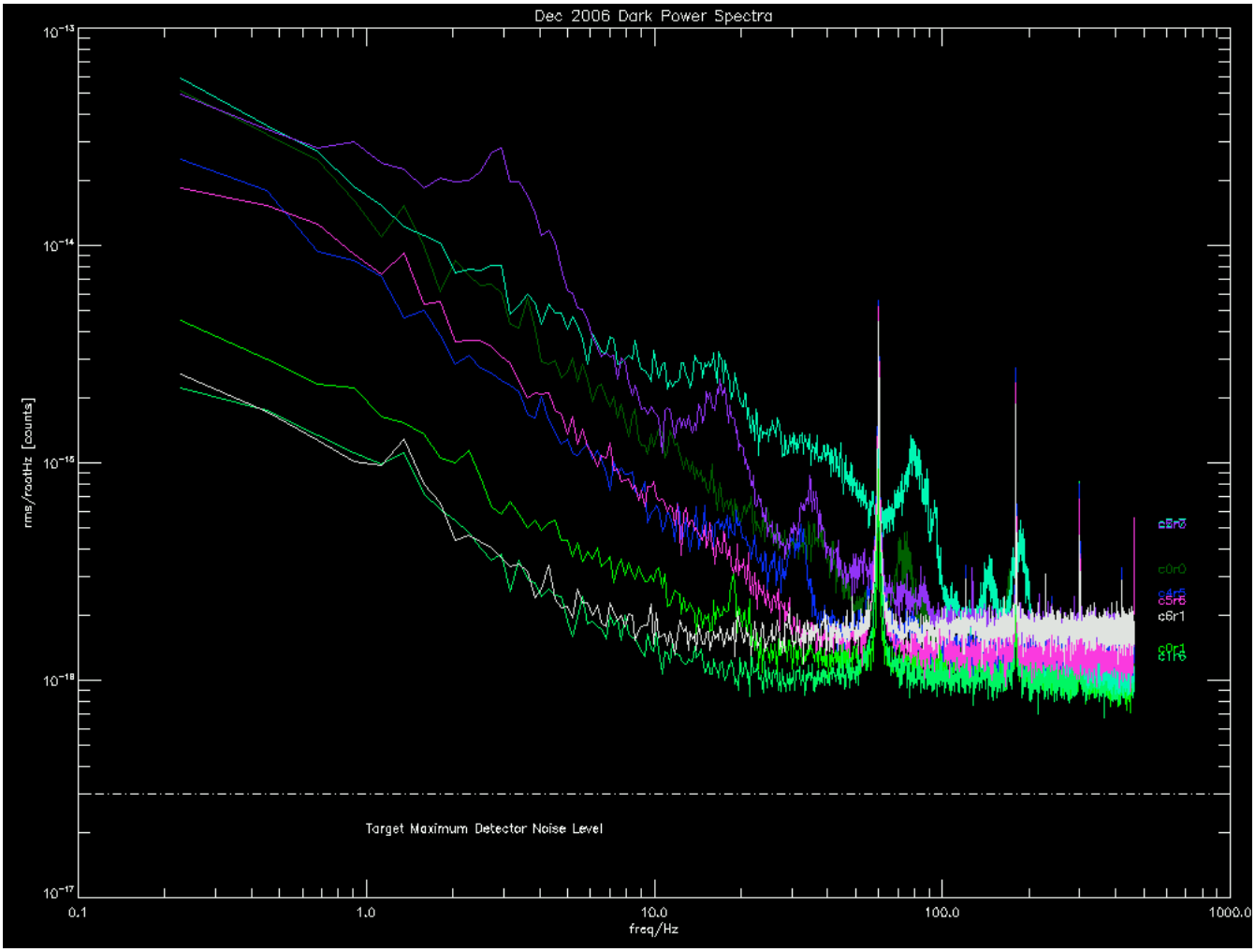

FIGURE 7: Noise Power spectra for the same set of pixels from the post-GBT 0.3 K dark run. Y-axis again is Watts rtHz.

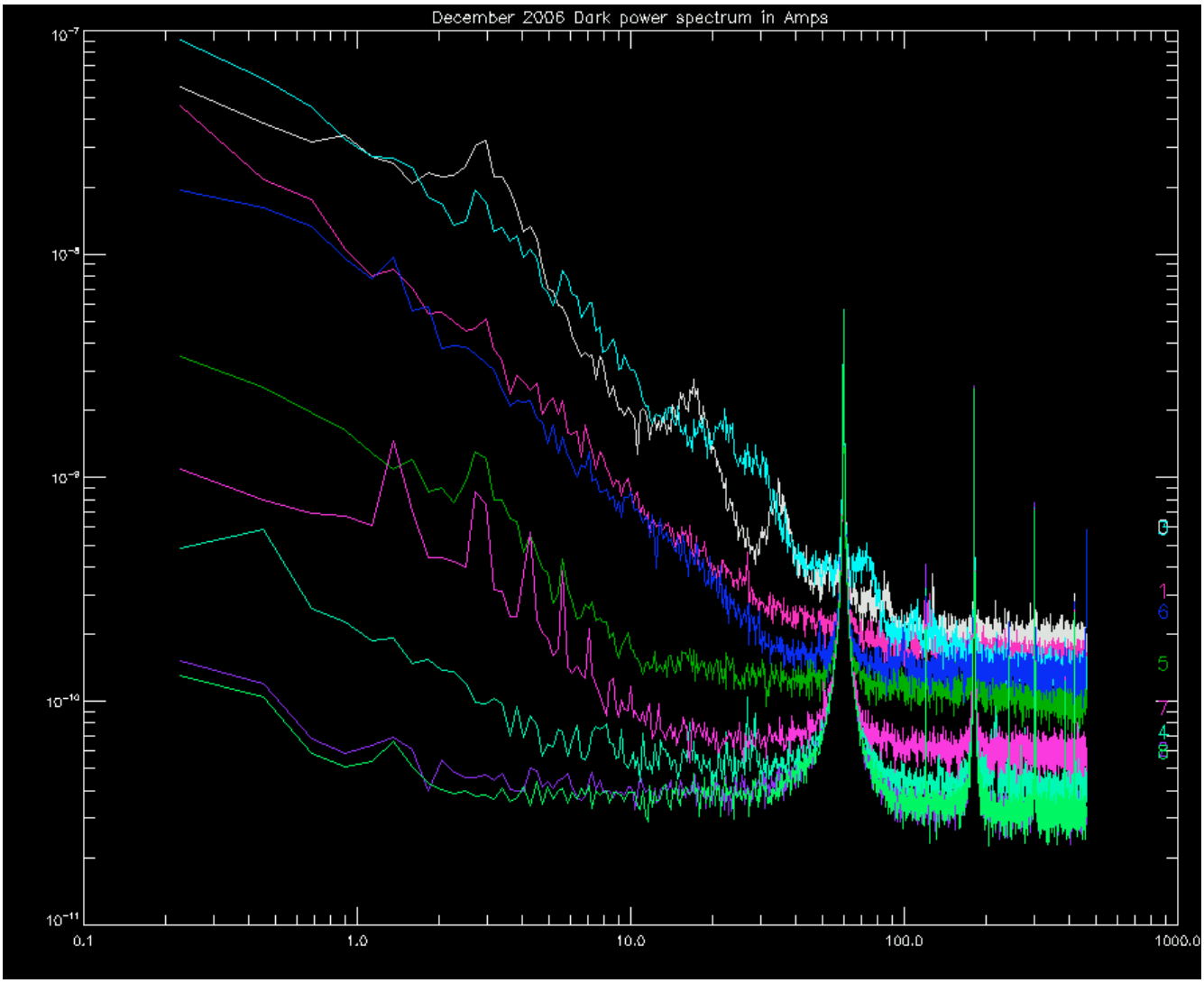

FIGURE 8: Power spectra for all rows in column 5 from the post-GBT 0.3K Dark run, this time in Amps rtHz.

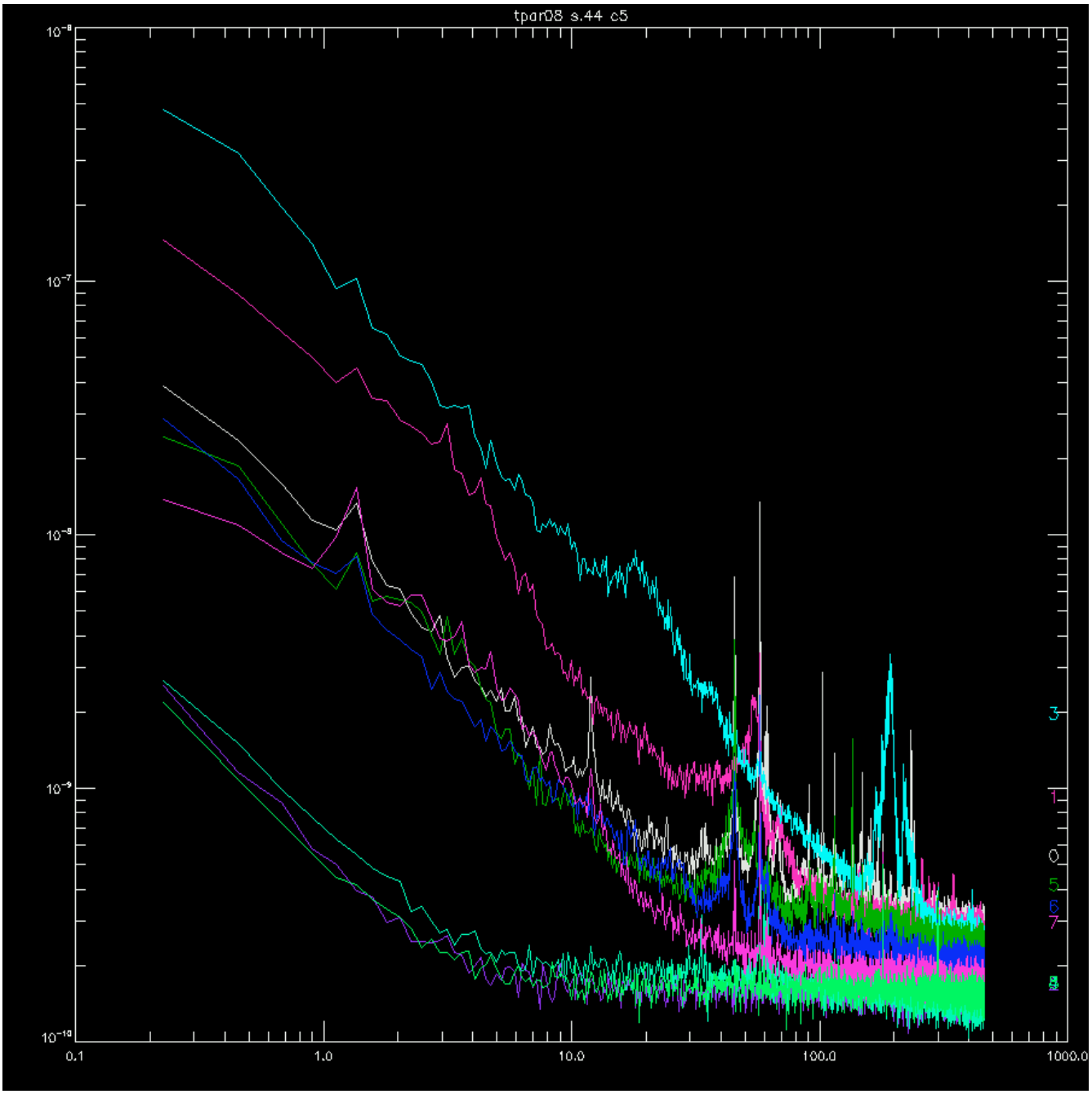

FIGURE 9: Power spectra from on the telescope (TPAR08), all rows in Column 5, in Amps rtHz.

Comments:

- The high-frequency current noise floor on the telescope seems higher than in the lab (figs 9 vs 8). Is this real, and if so, what is the reason?

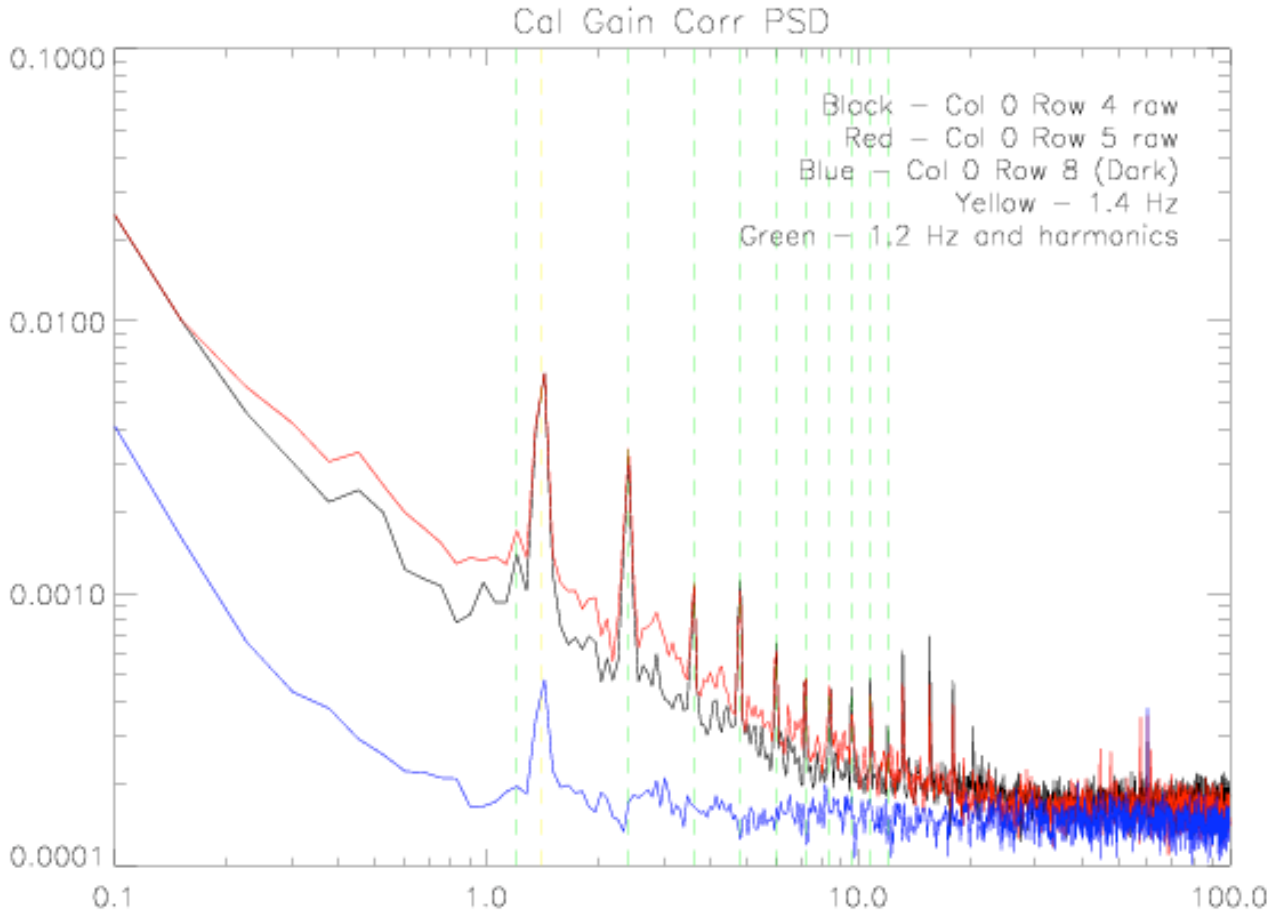

FIGURE 11: Noise power spectra for two pixels (c0r4 and c0r5) plus the dark squid from C0, showing effects due to GBT and MUSTANG fridges. The stepper motor for the MUSTANG fridge operates at 1.4 Hz and is evident in the dark squid as well as the detectors, indicating that there is a thermal coupling. The GBT fridges operate at 1.2 Hz and harmonics of this from 2.4 Hz on up are clearly evident only in the detector data, indicating a microphonic effect (seen to be intermittent).

6.2 Noise Correlations

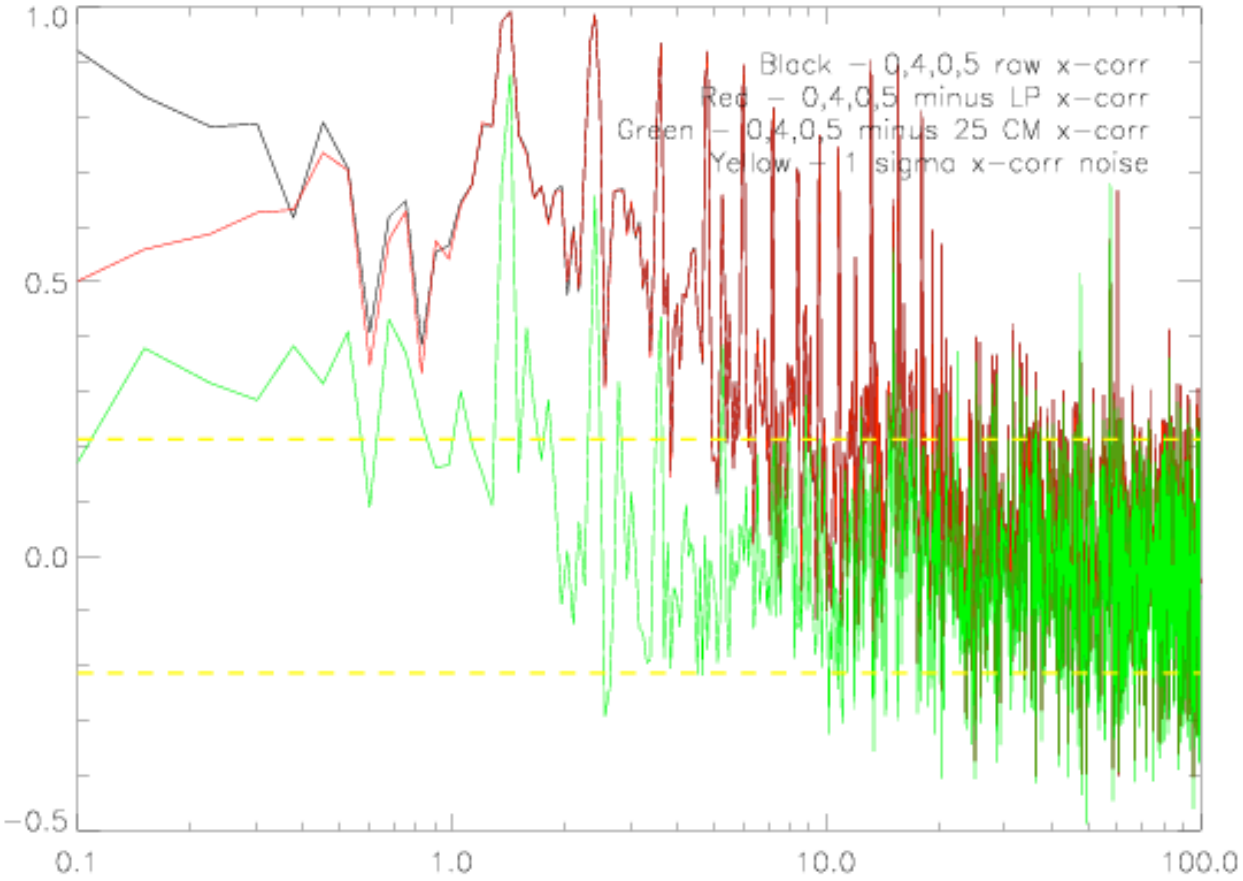

FIGURE 12: Cross power spectra for c0r4/c0r5 with a variety of data filtering strategies. Black is the raw cross power spectrum; red is the cross power spectrum after individual low-pas subtraction; green is the cross power spectrum after a 25-good-pixel common mode subtraction. Yellow lines are +/- 1 sigma stsatistical uncertainties on the estimates of individual cross-spectrum coefficients. These spectra are normalized by the autocorrelations to lie in the range +/-1. The fact that the green line is consistent with zero, roughly, above a couple of Hz indicates that the medium frequency correlations between c0r4 and c0r5 are well represented by the 25-pixel common mode. There is a significant correlation between c0r4 and c0r5 at frequencies less than 2 Hz which is not well-represented by the 25-pixel common mode.

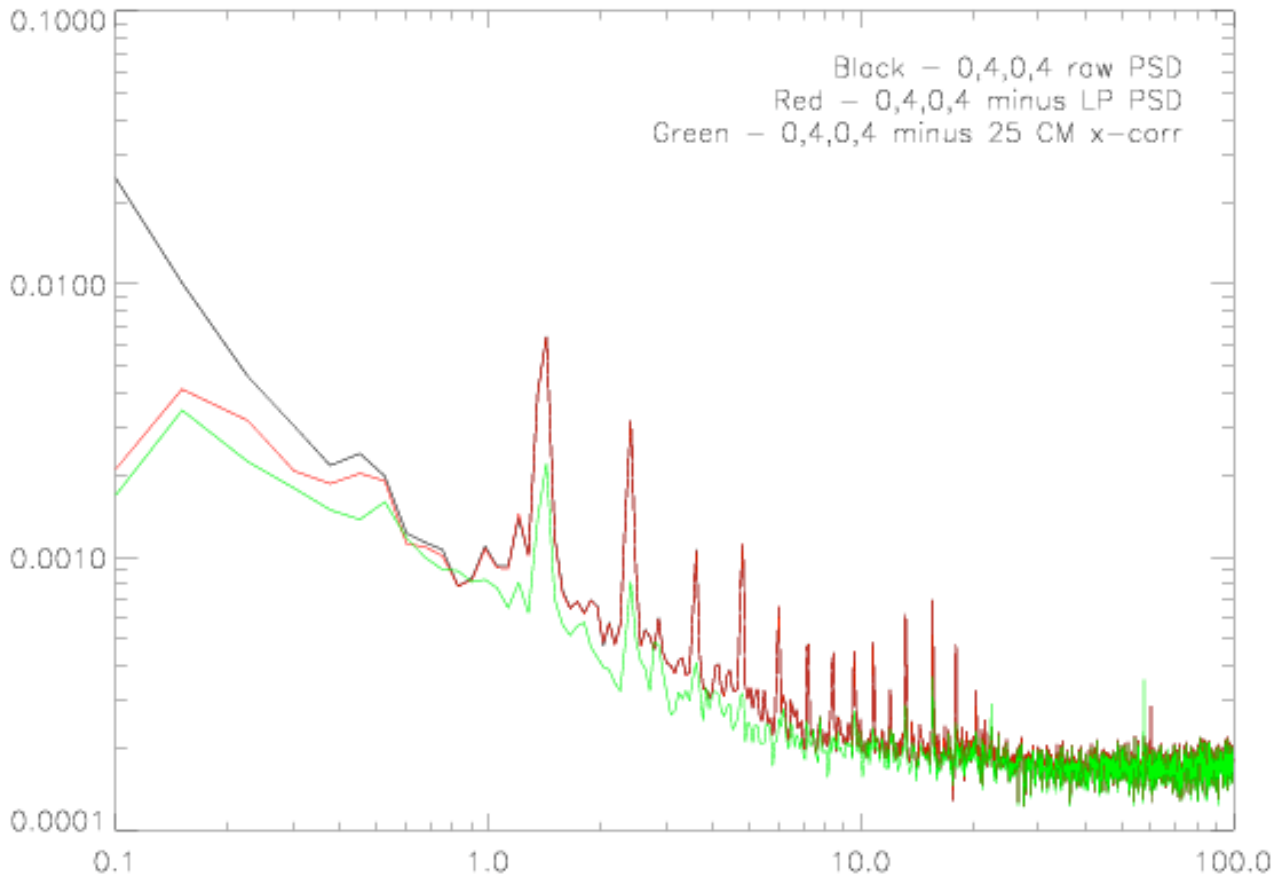

FIGURE 13: Noise power spectra for c0r5: raw (black); after low-pass filter subtraction (red); after 25-pixel common-mode subtraction (green). The fact that 1/f in the red and green traces remains, while the cross-correlations between c0r4 and c0r5 above 1 Hz are pretty small, is indicitave of uncorrelated 1/f noise.

7. Isolated Data Glitches (Cosmic Rays?) and Time Constants

A close inspection of the data reveals occasional large-amplitude, isolated spikes in the data (meaning they occur in one detector at a time). An example is shown in the following Figure. These could be cosmic ray hits; the ampltidue is typically on the order of one cal (1.2V) which is enormous--- Saturn is typically 0.6 cals. Fitting these events to a function of the form $e^{-t/tau}$ consistently gives tau=2.5 millisecond time constants. This is comparable to, but less than, the tau=5 ms lab-measured time constants.

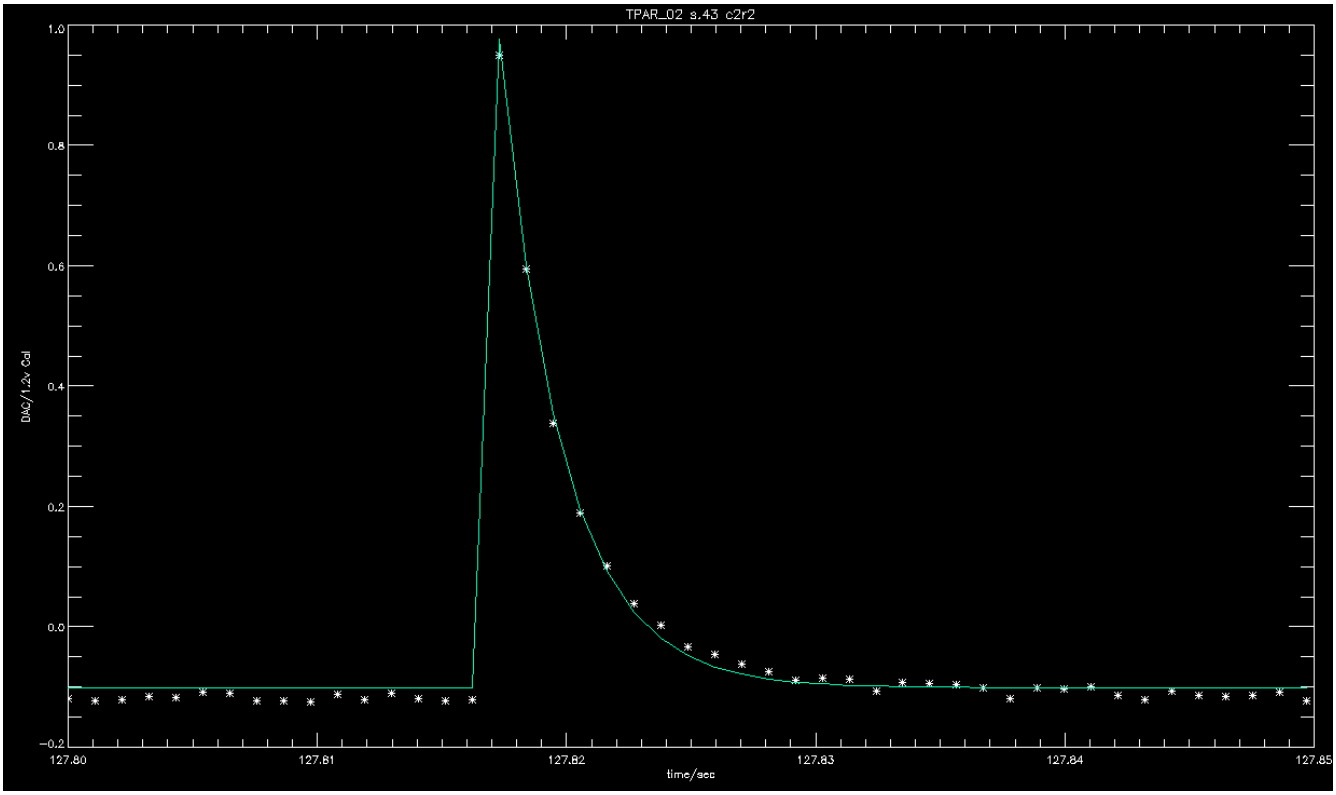

FIGURE 14: decaying exponential fit to a typical glitch event (2.5 ms time constant)

8. GBT 3mm Surface Efficiency

Following is Simon's calculation of the GBT 90 GHz optical efficiency from MUSTANG data.

Assume:

1: Saturn is a black body at Ts=130K 17.5" by 14.0" in diameter

2: The used surface on the gbt is 45m raduis

3: Our detectors ar 3.3mm square with an f 1.62 focus

4: Our bandpass is 86-94 GHz

1: how much in-band power does a perfect gbt receive from saturn in zero opacity conditions?

The intergral of a black body across our band is 2.554e-6 W/m^2/rad multiply this by the area of the primary and the angular diameter of saturn to get that the total amount of power arriving from saturn is 73.5pW (look in saturn2.pro for details).

2:Calculate the shape of an image of saturn on the focal plane. I did this using IDL program saturn.pro. First calculate a beamshape assuming tophat illumination of a 45m radius mirror at a wavelength of 3.3mm. then convolve this with an elipse 17.5" by 14".

3:integrate to find the fraction of the power in the image of saturn in a 3.3mm square detector = 8.2% (done in saturn.pro). From this we can say the total amount of power a detector should see from saturn is:

6.01pW * cryostat optical efficency * surface efficiency * atmosphere

4:The best measurements for the cryostat optical efficency are 30% (done with hot/cold load tests and detector bias curves)

5:The optical transmision of the atmosphere is exp(-tau/sin(elevation)). Tau was obtained from weather records as sky dips did not give a good fit.

6:From T_PAR02 it is estimated Saturn came through at 0.15pW, Tau = 0.13 and the elevation was 44 degrees 6.01*0.3*exp(-0.13/sin(44)) = 1.5pW if the surface efficency was 100% => 10% surface efficiency

7:the same method for T_PAR05 gives 1.32 expected, 0.1pw observed (scan 109) and 0.126pw observed (scan 122) to give surface efficiencies of 7.25 and 9.5%

8. Images & Data Reduction

All mustang data were collected in an on-the-fly mapping mode, which keeps scan-start overheads and related potential problems (e.g., feedarm ringing) to a minimum, and spreads coverage of a given sky pixel between numerous detectors, aiding in image reconstruction. To make images from our commissioning data, we followed a simple procedure:

- from the GBT indicated positions (RA,Dec) and previously measured per-detector beam offsets (El, cross-Elevation), calculate the Ra and dec of each detector as a function of time through the scan.
- Subtract a baseline. We experimented with two subtraction techniques: a per-integration common mode (average of "good" pixels), and a per-detector low-order polynomial determined in an off-source region of the map and subtracted from the entire timestream. The former most effectively subtracts atmospheric and instrumental noise, but introduces artifacts around bright sources.
- Grid the resulting cleaned timestream data, detector by detector, onto the sky. A simple cloud-in-cloud (bilinear interpolation) was used with pixels 1-4 arcsec in size.

These procedures were implemented in IDL and made use of code generously provided by Ed Chapin & David Hughes of INAOE. Bill Cotton also modified his package OBIT to analyze MUSTANG data. OBIT uses an iterative CLEAN-like algorithm to construct a sky model (see Figure 17).

To quantify the noise levels in our data we consider TPAR_05 scan 79, a 6-minute daisy scan covering 1/3 of a 4' radius circle centered on 3c84. These data and the maps that result are typical. We find an RMS of 0.3 Jy. Allowing for the GBT surface (a factor of 3 from its target 30% efficiency), the number of detectors functioning (33), and the excess in the individual-detector noise levels (about 300), this noise level is what is expected.

Following are several maps from the commissioning run.

Figure 15: GBT+MUSTANG first light image of Saturn. The apparent elongation of the image is due to a cos(elevation) error in the analysis software since corrected.

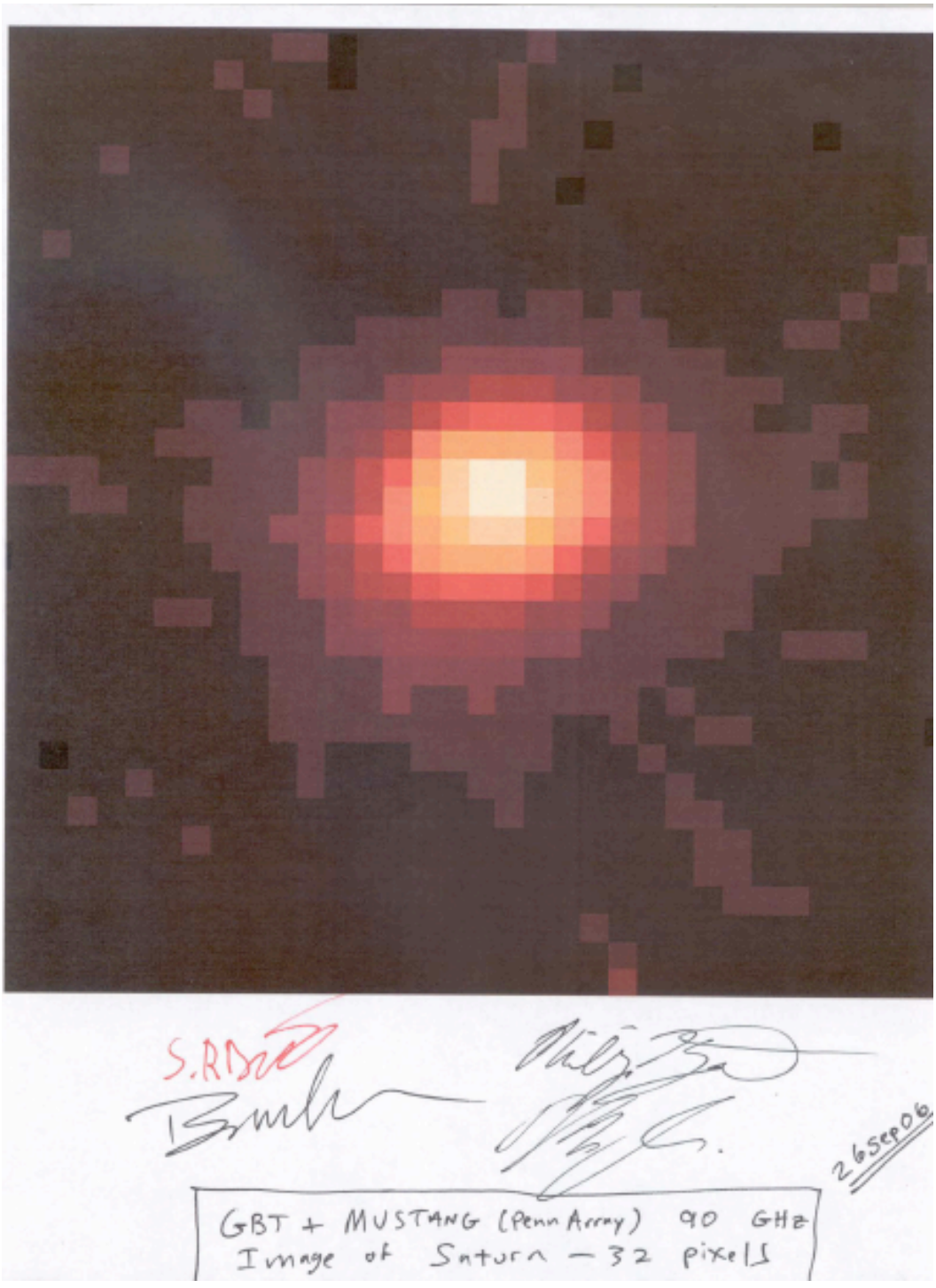

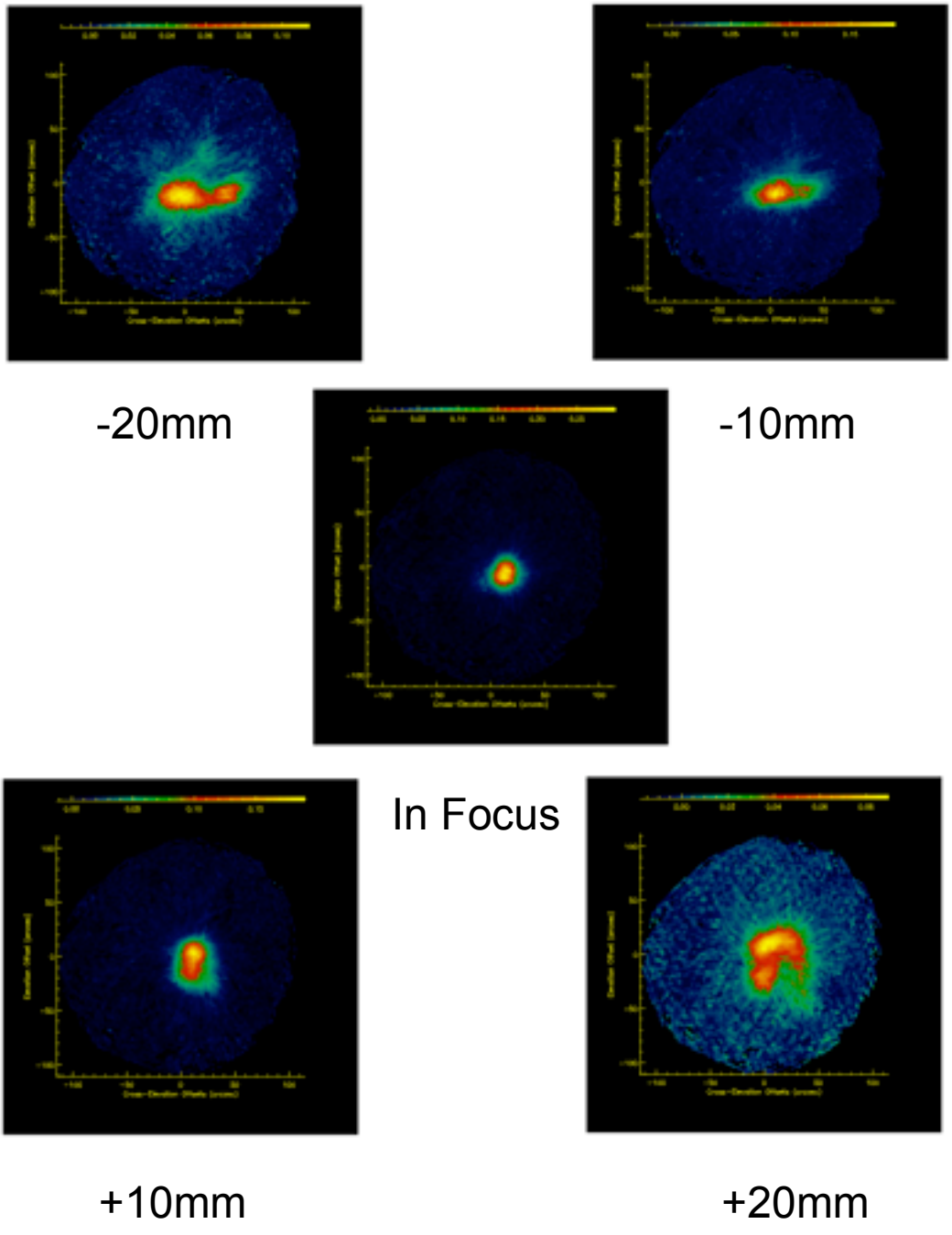

Figure 16: GBT+MUSTANG maps of Saturn collected at 5 distinct y-axis focus settings.

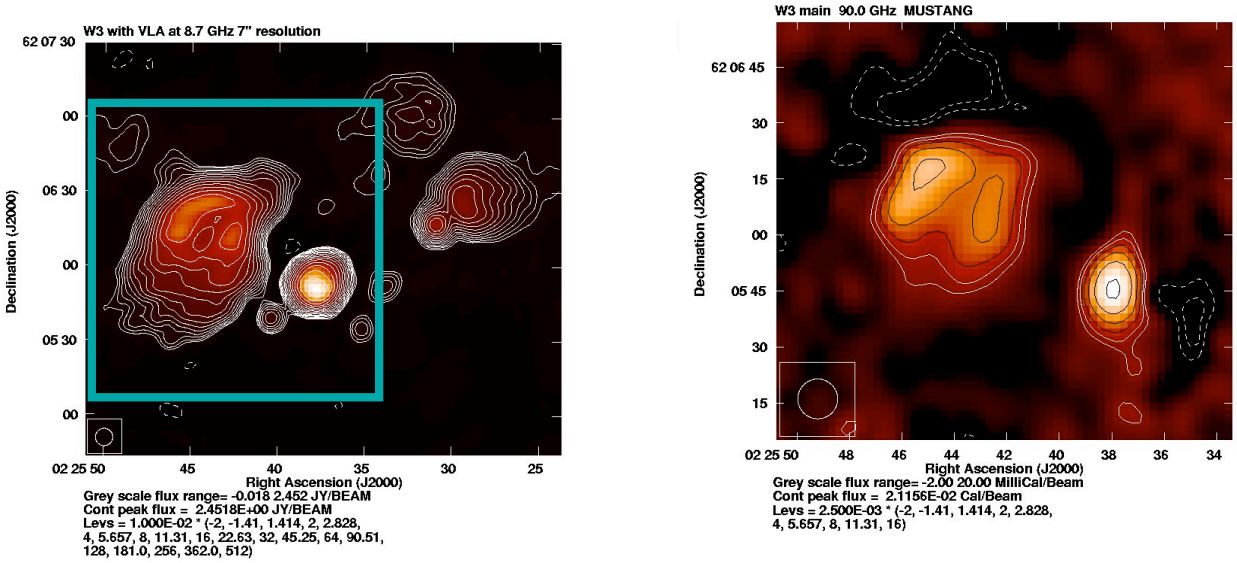

Figure 17: VLA 8 GHz (left) and MUSTANG 3mm maps of W3main (MUSTANG map is of the boxed region in the VLA image). Both images courtesy of Bill Cotton.

9. Conclusions & Areas for Further Work

In light of the difficulty of the measurements, MUSTANG performed admirably on the GBT. The GBT itself is seen to have roughly the expected 10% aperture efficiency; since it is outfitted with a fully functional active surface, we expect outstanding 3mm performance will be reached in the near future.

Outstanding issues, needing further investigation, are:

- 1/f noise (probably in the detectors themselves)
- Detector consistency & functionality (better than 50% working; more consistent noise characteristics of those that see light).
- Intrinsic detector noise floor at high frequency is more than 3x over our maximum target; and we don't see photon noise at all (hot vs cold load)
- Improve cryogenic performance, and in particular, recovery time from long dwells at low elevation ranges.
- Mitigate GBT-fridge microphonics